Stimulated Emission Depletion Studies of Molecular Probe Dynamics.

R J Marsh, N D Leonczek, D A Armoogum, E M Monge and A J Bain[+]

Department of Physics & Astronomy, University College London, Gower Street, London WC1E 6BT, UK
[+]Corresponding Author.

ABSTRACT

Stimulated emission depletion (STED) population and polarisation dynamics are used to determine $\langle \alpha_{40} \rangle$ the degree of hexadecapole alignment created in ensembles of rhodamine 6G molecules in solution following two-photon excitation. Hexadecapole molecular alignment is an unavoidable consequence of two-photon excitation but is not observed in spontaneous emission. For a single element diagonal transition tensor measurements of the fluorescence anisotropy $R(t)$ in systems undergoing small step isotropic rotational diffusion can in principle be used to determine $\langle \alpha_{40} \rangle$. STED measurements of rhodamine 6G yield a value for $\langle \alpha_{40} \rangle$ that is larger than that predicted for a single element transition tensor (S_{XX}). Recent work in our laboratory indicates that whilst S_{XX} is dominant S_{YY}, S_{XY} and S_{YX} are finite, measurements of $\langle \alpha_{40} \rangle$ appear to be a sensitive probe of the structure of the two-photon transition tensor. STED and fluorescence anisotropy measurements are extended to Rhodamine 6G in the isotropic phase of 5CB a system where small step isotropic rotational relaxation does not take place. Here the values of $\langle \alpha_{40} \rangle$ are considerably larger. These results are discussed in terms of the initial hexadecapole alignment and $\langle \alpha_{40} \rangle$ relaxation dynamics in a restricted geometry.

Key words: Stimulated emission depletion, two-photon fluorescence, molecular alignment, polarisation, transition tensor.

1. INTRODUCTION

Stimulated emission depletion (STED) of excited states has proved to be both a valuable tool in high resolution molecular spectroscopy[1], in time resolved spectroscopy as a means of orientational photoselection[2] and in the study of ultrafast vibrational relaxation within electronic ground states[3]. There has been considerable interest in the use of single photon STED in fluorescence microscopy[4] where sub wavelength image resolution has been recently demonstrated[5]. Recent work in our laboratory[6-10] has demonstrated the feasibility of performing STED in two-photon excited states. In this work femtosecond near infra red (800nm) two-photon excitation (PUMP) is followed by visible picosecond stimulated emission depletion (DUMP) of the excited state. Time-resolved fluorescence detection is employed to determine changes in excited state population and alignment following STED together with the measurement of stimulated emission cross-sections and ground state vibrational relaxation times. Measurements of fluorescence anisotropy changes induced by STED are sensitive to higher degrees of excited state order and as such can be used to circumvent the constraints of single photon emission which are sensitive solely to molecular alignment (quadrupolar order). In this paper we determine absolute values for the normally hidden degrees of hexadecapolar molecular alignment created by two-photon excitation of rhodamine 6G in ethylene glycol and the isotropic phase of 5CB.

2. POLARISED STIMULATED EMISSION DEPLETION

A schematic representation of the two-photon STED process in rhodamine 6G is shown in Figure 1. Initial excitation from low lying vibrational levels in the S_0 ground state occurs via the simultaneous absorption of two (non-resonant) near infra red photons with fast radiationless conversion yielding a vibrationally excited population in the S_1 excited electronic state. Fast collisional (and solvent) relaxation leads to the rapid population of lower vibrational levels in S_1. In the absence of external perturbations the population in S_1 decays by spontaneous emission to upper vibrational levels of S_0 followed by rapid collisional deactivation. In STED a visible laser pulse resonant with the $S_1 \rightarrow S_0$ emission is applied to induce transitions to upper vibrational levels of S_0. The net result of this process is a sharp reduction in the excited state population (fluorescence intensity) and a change in molecular alignment (fluorescence anisotropy) dependent on the relative polarisation of the two laser pulses. Depletion of the excited state is maximised for parallel PUMP and DUMP polarisations and at PUMP-DUMP delays that are short in comparison to the rotational diffusion time of the molecule[6-10]. STED dynamics can be modelled analytically in the limit of fast ground state relaxation and weak depletion of the excited state population. For strong saturation of the DUMP transition analytic solutions to the coupled rate equations are possible for model DUMP pulse shapes[6,7].
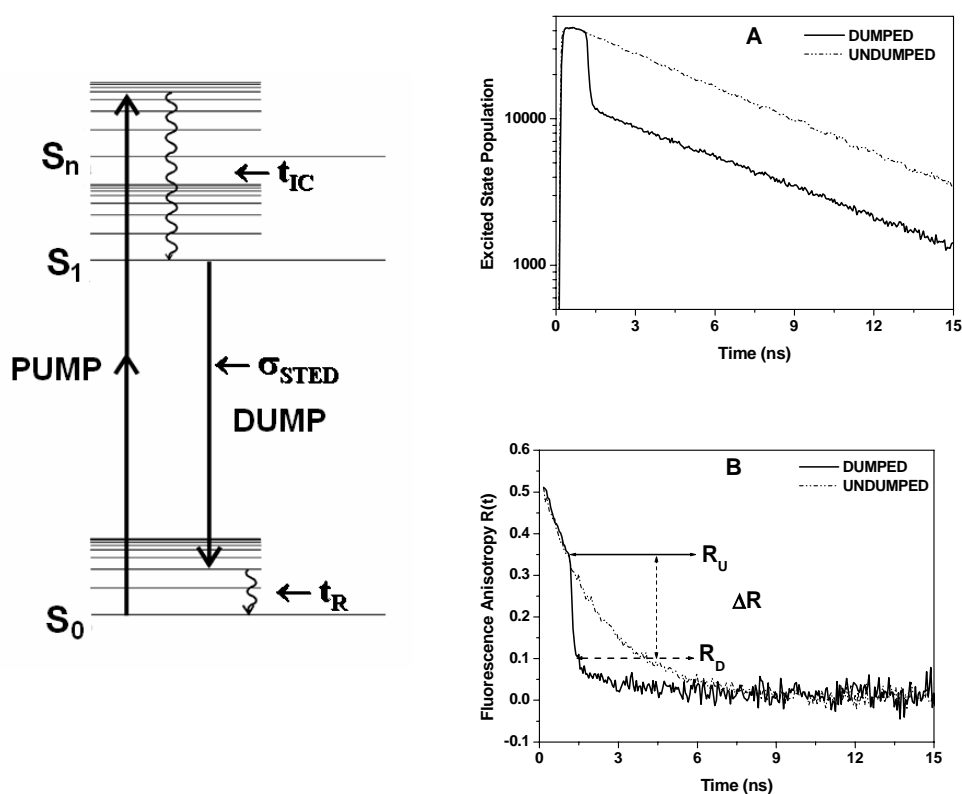

Figure 1: Stimulated emission depletion (STED) in rhodamine 6G. Linearly polarised two-photon excitation (PUMP) is followed by a time delayed (1ns, 17nJ, 622nm) DUMP pulse. With parallel PUMP and DUMP polarisations both population (A) and alignment (B) reductions are maximised. The reductions in the excited state population and alignment are 70% and 0.23 respectively

3. PHOTOSELECTION IN TWO-PHOTON EXCITATION

Excited State Orientational Distribution

In experiments involving optical probes of molecular order and motion in fluid media it is advantageous to adopt a formalism in which the inherent symmetry of the radiation-molecule interaction and those of the experimental observables are fully exploited. To this end an expansion of the molecular orientational distribution function in terms of spherical harmonics has been widely used[11-13]. In the polar coordinate system in Figure 1, the probability of finding a molecule with an orientation between the polar angles θ and $\theta+d\theta$, ϕ and $\phi+d\phi$ is given by

$$P(\theta,\phi) = \sum_{KQ} \langle C_{KQ} \rangle Y_{KQ}(\theta,\phi) \tag{1}$$

where the expansion coefficients $\langle C_{KQ} \rangle$ define the moments of the distribution and can be found from (1) using the orthogonality of spherical harmonics,

$$\langle C_{KQ} \rangle = \int_0^{2\pi}\int_0^{\pi} Y_{KQ}^*(\theta,\phi) P(\theta,\phi) \sin\theta d\theta d\phi \tag{2}$$

The probability of finding a molecule in any orientation on the unit sphere is necessarily unity, thus

$$\sum_{KQ} \langle C_{KQ} \rangle \int_0^{2\pi}\int_0^{\pi} Y_{KQ}^*(\theta,\phi) \sin\theta d\theta d\phi = \sum_{KQ} \langle C_{KQ} \rangle \sqrt{4\pi} \delta_{K0} \delta_{Q0} = 1 \tag{3}$$

giving a constant population moment (or monopole) $\langle C_{00} \rangle = 1/\sqrt{4\pi}$ The orientational probability can also be expressed in terms of normalised moments, $\langle \alpha_{KQ} \rangle = \langle C_{KQ} \rangle / \langle C_{00} \rangle$

$$P(\theta,\phi) = \left[1 + \sqrt{4\pi} \sum_{K \rangle 0, Q} \langle \alpha_{KQ} \rangle Y_{KQ}(\theta,\phi) \right] \Big/ 4\pi \tag{4}$$

The multipole moments $\langle \alpha_{KQ} \rangle$ are directly related to measurable experimental quantities; moreover their transformation properties upon a change in coordinate system are particularly suited to fluorescence polarisation experiments[14,15]. In the weak excitation limit with a short pulsed optical excitation in an isotropic medium the moments of the initial excited state distribution are given by,

$$\langle \alpha_{KQ} \rangle = \left[\int_0^{2\pi} d\phi \int_0^{\pi} Y_{KQ}(\theta,\phi)^* W_{EX}(\theta,\phi) \sin\theta d\theta \right] \Big/ \left[\int_0^{2\pi} d\phi \int_0^{\pi} Y_{00}(\theta,\phi)^* W_{EX}(\theta,\phi) \sin\theta d\theta \right] \tag{5}$$

where $W_{EX}(\theta,\phi)$ is the angle dependent transition probability in the laboratory frame. The transition probability for the absorption of two photons of polarisations α and β between states i and f is proportional to the squared modulus of the tensor $W_{\alpha\beta}^{i \to f}$ defined by a sum of transitions involving intermediate (virtual) states n[16]

$$W_{EX}^{TPA}(\theta,\phi) \equiv \left| W_{\alpha\beta}^{i \to f} \right|^2 = \left| \sum_n \left(\frac{\alpha \cdot \langle i|r|n\rangle\langle n|r|f\rangle \cdot \beta}{\upsilon_n - \upsilon_\alpha + i\Gamma_n} + \frac{\beta \cdot \langle i|r|n\rangle\langle n|r|f\rangle \cdot \alpha}{\upsilon_n - \upsilon_\beta + i\Gamma_n} \right) \right|^2 \tag{6}$$

where υ_n and Γ_n are the transition frequency and homogeneous linewidth of n respectively. In the molecular frame of reference the transition tensor can have 9 elements S_{AB} where A, B=X, Y or Z.

$$\left| W_{\alpha\beta}^{i\rightarrow f} \right|^2 \equiv \left| \sum_{A,B=X,Y,Z} S_{AB} \right|^2 \tag{7}$$

For planar aromatic molecules the two-photon transition is dominated by moments in the plane of the molecule[17-19] and the summation over Z can be neglected. For degenerate two-photon absorption with linearly polarised light $S_{AB}=S_{BA}$ and $\alpha = \beta$. Photoselection in the laboratory frame is necessarily cylindrically symmetric about α and the excited state multipole moments are restricted to Q=0. Further symmetry and angular momentum constraints inherent in the matrix elements of (6) restrict the rank K to even integers with a maximum rank of K=4. As a result the initial excited state distribution function is characterised solely by $\langle \alpha_{20} \rangle$ and $\langle \alpha_{40} \rangle$

$$P(\theta,\phi,t=0) = \frac{\left[Y_{00}(\theta,\phi) + \langle \alpha_{20}(0) \rangle Y_{20}(\theta,\phi) + \langle \alpha_{40}(0) \rangle Y_{40}(\theta,\phi) \right]}{\sqrt{4\pi}} \tag{8}$$

Where the transition is largely dominated by S_{XX} the laboratory frame transition probability approximates to $cos^4\theta$ where θ is the angle between the laboratory Z axis and the X axis of the transition tenor which is taken to be the direction of the emission transition dipole moment. Under these circumstances (8) becomes

$$P(\theta,\phi,t=0) = \frac{1}{\sqrt{4\pi}} \left[Y_{00}(\theta,\phi) + \frac{4\sqrt{5}}{7} Y_{20}(\theta,\phi) + \frac{8}{21} Y_{40}(\theta,\phi) \right] \tag{9}$$

Polar plots of the angular contributions to $P(\theta,\phi)$ are shown in figure 2.

$$P(\theta,\phi,t) = \frac{\left[Y_{00}(\theta,\phi) + \langle \alpha_{20}(t) \rangle Y_{20}(\theta,\phi) + \langle \alpha_{40}(t) \rangle Y_{40}(\theta,\phi) \right]}{\sqrt{4\pi}}$$

$$\left(\frac{5}{8\pi}\right)^{\frac{1}{2}} (3\cos^2\theta - 1) \qquad \left(\frac{9}{64\pi}\right)^{\frac{1}{2}} (35\cos^4\theta - 30\cos^2\theta + 3)$$
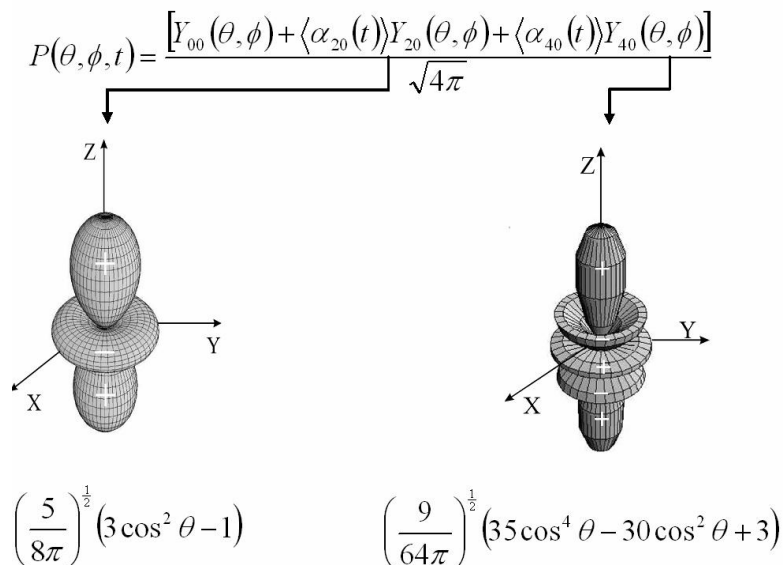
Figure 2: Angular contributions to the excited state orientational distribution prepared by two-photon excitation.

The parallel and perpendicular components of the fluorescence anisotropy are given by

$$I_{\parallel}(t) \propto N_{ex}(t=0) \int\limits_0^{2\pi}\int\limits_0^{\pi} P(\theta,\phi,t=0)\cos^2\theta\sin\theta\, d\theta d\phi$$

$$I_{\perp}(t) \propto N_{ex}(t=0) \int\limits_0^{2\pi}\int\limits_0^{\pi} P(\theta,\phi,t=0)\sin^2\theta\cos^2\phi\sin\theta\, d\theta d\phi$$

(10)

Expressing the parallel and perpendicularly polarised emission transition probabilities in terms of spherical harmonics yields

$$I_{\parallel}(t=0) \propto N_{ex}(t=0) \int\limits_0^{2\pi}\int\limits_0^{\pi} P(\theta,\phi,t=0)\left[Y_{00}(\theta,\phi)+\frac{2}{\sqrt{5}}Y_{20}(\theta,\phi)\right]\sin\theta\, d\theta d\phi$$

$$I_{\perp}(t=0) \propto N_{ex}(t=0) \int\limits_0^{2\pi}\int\limits_0^{\pi} P(\theta,\phi,t=0)\left[\begin{array}{c}Y_{00}(\theta,\phi)-\dfrac{1}{\sqrt{5}}Y_{20}(\theta,\phi)\\[2mm] +\left(\dfrac{3}{10}\right)^{\frac{1}{2}}(Y_{22}(\theta,\phi)+Y_{2-2}(\theta,\phi))\end{array}\right]\sin\theta\, d\theta d\phi$$

(11)

From the orthogonality of the spherical harmonics only the K=2 rank moments of the excited state distribution can contribute to $I_{//}$ and $I_{\perp}$ and the initial fluorescence anisotropy becomes,

$$R(0) = \frac{I_{\parallel}(t)-I_{\perp}(t)}{I_{\parallel}(t)2I_{\perp}(t)} = \frac{\langle\alpha_{20}(0)\rangle}{\sqrt{5}} = \frac{4}{7}$$

(12)

For a molecular array with 100% alignment $P(\theta,\phi)=\delta_{\theta 0}\delta_{\phi 0}$ and the moments of the distribution function are given by

$$\left\langle \alpha_{KQ}{}^{MAX}\right\rangle = \sqrt{(2K+1)}\delta_{Q0}$$

(13)

The maximum permissible values of $\langle\alpha_{20}\rangle$ and $\langle\alpha_{40}\rangle$ are $\sqrt{5}$ and 3 respectively.

4. TWO-PHOTON FLUORESCENCE ANISOTROPY

Homogeneous Isotropic Fluid Media

In isotropic fluid media molecular alignment following short pulse excitation is, in the case of small step rotational diffusion about a single molecular axis, governed by Debye diffusion dynamics[20]

$$\frac{\partial P(\theta,\phi,t)}{\partial t} = D\nabla^2 P(\theta,\phi,t)$$

(14)

where D is the diffusion coefficient for the molecule. Inserting (1) into 14 yields

$$\sum_{KQ}\frac{\partial}{\partial t}\langle C_{KQ}(t)\rangle Y_{KQ}(\theta,\phi) = \sum_{KQ}\langle C_{KQ}(t)\rangle D\nabla^2 Y_{KQ}(\theta,\phi)$$

(15)

The spherical harmonics $Y_{KQ}(\theta,\phi)$ are eigenfunctions of ∇^2 with eigenvalues $-K(K+1)$

$$\sum_{KQ}\frac{\partial}{\partial t}\left\langle C_{KQ}(t)\right\rangle Y_{KQ}(\theta,\phi)=-\sum_{KQ}\left\langle C_{KQ}(t)\right\rangle DK(K+1)Y_{KQ}(\theta,\phi) \tag{16}$$

Multiplying by $Y_{K'Q'}(\theta,\phi)^*$ and integrating over the unit sphere (16) becomes

$$\frac{\partial}{\partial t}\left\langle C_{KQ}(t)\right\rangle=-DK(K+1)\left\langle C_{KQ}(t)\right\rangle \tag{17}$$

For small-step rotational diffusion to an isotropic steady state, the time dependence of $P(\theta,\phi)$ is thus

$$P(\theta,\phi,t)=\frac{1}{\sqrt{4\pi}}\left[Y_{00}(\theta,\phi)+\left\langle\alpha_{20}(t=0)\right\rangle\exp(-6Dt)Y_{20}(\theta,\phi)+\left\langle\alpha_{40}(t=0)\right\rangle\exp(-20Dt)Y_{40}(\theta,\phi)\right] \tag{18}$$

From (12) the time-dependent fluorescence anisotropy is thus

$$R(t)=\left(\left\langle\alpha_{20}(t=0)\right\rangle/\sqrt{5}\right)\exp(-6Dt)\equiv R(0)\exp(-t/\tau_{20}) \tag{19}$$

The K=4 orientational dynamics do not contribute to $R(t)$ but, as will be seen, the presence of hexadecapole alignment plays a significant role in stimulated emission dynamics. From (18) and (19) it is possible to predict the relative decay of the hexadecapole alignment from the change in fluorescence anisotropy,

$$R(t)/R(0)=\exp(-t/\tau_{20}),\quad\left\langle\alpha_{40}(t)\right\rangle/\left\langle\alpha_{40}(0)\right\rangle=\exp(-10t/3\tau_{20}) \tag{20}$$

which yields

$$\left[\left\langle\alpha_{40}(t)\right\rangle/\left\langle\alpha_{40}(0)\right\rangle\right]=\left[R(t)/R(0)\right]^{\frac{10}{3}} \tag{21}$$
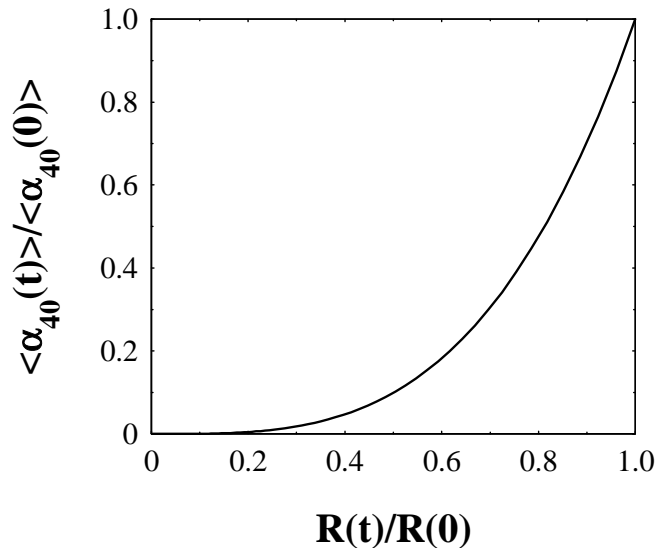

Figure 3: Variation in hexadecapole alignment with the decay of molecular alignment (fluorescence anisotropy) assuming small step isotropic rotational diffusion.

Rotational Diffusion in Liquid Crystals

Compared to the single exponential decay that characterises single axis probe diffusion in homogeneous isotropic liquids, in liquid crystals the fluorescence anisotropy whilst decaying to zero (the medium being globally isotropic) is characterised by fast but restricted (incomplete) intra-pseudodomain rotational diffusion (τ_{20}^F) mediated by a slower overall orientational averaging (τ_{20}^S) of the pesudodomain structure[21]. This behaviour has been observed in both single and two-photon fluorescence anisotropy studies of fluorescent probe motion in the isotropic phase of 5CB[22]. Interpretation of the probe anisotropy decays can be undertaken using the model of restricted rotational diffusion within a cone from which a local order parameter $\left\langle \alpha_{20}^M \right\rangle$ can be extracted.

$$R(t) \cong R(0)\exp\left(-t/t_{20}^S\right)\left[\left(1-\left(\left\langle \alpha_{20}^M \right\rangle \middle/ \sqrt{5}\right)^2\right)\exp\left(-t/t_{20}^F\right)+\left(\left\langle \alpha_{20}^M \right\rangle \middle/ \sqrt{5}\right)^2\right] \tag{22}$$

In such instances Debye diffusion does not hold and the simple relationship between $\left\langle \alpha_{20} \right\rangle$ and $\left\langle \alpha_{40} \right\rangle$ evolution as expressed in (17)-(21) and illustrated in figure 4 does not hold. In a highly structured local environment the divergence in τ_{40}^F and τ_{20}^F from (18) should be marked.

4 POPULATION AND ALIGNMENT DYNAMICS IN STED

Weak Depletion Limit

The contribution of the degrees of excited state alignment to STED observables can be highlighted in the limit of weak excited state depletion and fast ground state relaxation. The relationship between the initial (undumped) and final (dumped) orientational probability distribution functions being given by[7],

$$P_D(\theta,\phi) = \frac{N_U}{N_D}P_U(\theta,\phi)\left[1 - SW_D(\theta,\phi)\right] \tag{23}$$

$P_U(\theta,\phi)$, N_U, N_D and $P_D(\theta,\phi)$ are respectively the undumped (initial) and dumped (final) excited state populations and orientational distribution functions, $W_D(\theta,\phi)$ is the angular dependent DUMP transition probability and S is the saturation parameter for the transition given by $S = \sigma E/h\nu A$ where σ is the stimulated emission cross-section, A is the beam area, E and $h\nu$ are the DUMP pulse and photon energies respectively. Expressing the orientational distribution functions as in (1), the moments of the altered distribution for parallel PUMP and DUMP polarisations are

$$\left\langle C_{KQ}^D \right\rangle = \frac{N_U\sqrt{4\pi}}{3N_D}\sum_{K'Q'}\left\langle C_{K'Q'}^U \right\rangle \left\langle KQ \middle| \left((3-S)Y_{00}(\theta,\phi) + \frac{2}{\sqrt{5}}SY_{20}(\theta,\phi) \right) \middle| K'Q' \right\rangle \tag{24}$$

The superscripts U and D refer respectively to the distributions immediately prior to and after the application of the DUMP pulse. Evaluation of the matrix elements for the directly observable moments of the altered array $\left\langle C_{00}^D \right\rangle$ and $\left\langle C_{20}^D \right\rangle$[7] yields analytic solutions for the fractional population removal F_D and the change in the fluorescence anisotropy ΔR

$$F_D = S(1+2R_U)/3 \tag{25}$$

$$\Delta R = R_U - R_D = S\left[\frac{2}{5} + \frac{4}{7}R_U - 2R_U^2 + \frac{12}{35}\left\langle \alpha_{40}^U \right\rangle\right]\middle/\left[3-(1+2R_U)S\right] \tag{26}$$

Here $\left\langle \alpha_{40}^U \right\rangle$ and R_U are respectively the normalised degree of hexadecapole alignment and the fluorescence anisotropy prior to excited state depletion. From (25) and (26) it can be seen that to first order the excited state depopulation

depends solely on the incident photon flux (via *S*) and the initial degree of alignment (via R_U), the depolarisation of the excited state additionally depends on the hexadecapolar degree of excited state alignment. In STED experiments involving significant excited state depopulation and depolarisation the departure from first order behaviour is marked. Nonetheless as will be seen ΔR saturation dynamics are considerably more sensitive to hexadecapolar alignment than the variation in F_D with DUMP pulse energy.

Rate Equation Analysis

The rate equations for STED on a timescale that is fast compared to spontaneous emission (nanosecond to sub-nanosecond) and orientational relaxation (nanosecond) are given by[7]

$$\frac{dN_{EX}(\theta,\phi,t)}{dt} = -\frac{I_D(t)\sigma W_D(\theta,\phi)}{h\nu}(N_{EX}(\theta,\phi,t)-N_{GS}(\theta,\phi,t)) \tag{27}$$

$$\frac{dN_{GS}(\theta,\phi,t)}{dt} = \frac{I_D(t)\sigma W_D(\theta,\phi)}{h\nu}(N_{EX}(\theta,\phi,t)-N_{GS}(\theta,\phi,t)) - \frac{N_{GS}(\theta,\phi,t)}{t_R} \tag{28}$$

Where $N_{EX}(\theta,t)$ and $N_{GS}(\theta,t)$ are the ground and excited state populations, $I_D(t)$ is the DUMP pulse intensity, $W_D(\theta)$ is the anglular dependence of the DUMP probability, σ is the stimulated emission cross-section (cm^2) and t_R is the ground state vibrational relaxation time. It is possible to obtain analytic solutions to the rate equations by assuming a rectangular DUMP pulse with width t_P, which yield the fractional remaining population F_R as a function of $E_P\sigma/h\nu A$ for given ratios of t_P/t_R. Given that the initial population distribution in the upper ground state vibrational levels is negligible, the excited state population evaluated at $t= t_P$ is

$$N_{EX}(\theta,\phi,t_P) = \frac{N_{EX}(\theta,\phi,0)}{2d}exp\left(-\frac{1}{2}\left\{\frac{t_P}{t_R}+2S\,cos^2\,\theta+d\right\}\right)\left[\frac{t_P}{t_R}\left(e^d-1\right)+d\left(e^d+1\right)\right] \tag{29}$$

where the parameter d is given by

$$d = \sqrt{\left(t_P/t_R\right)^2+4S^2\cos^4\theta} \tag{30}$$

The fractional depletion of the excited state population F_D and the anisotropy change ΔR can be calculated from

$$F_D = \int_0^{2\pi}\int_0^{\pi}[N_{EX}(\theta,\phi,0)-N_{EX}(\theta,\phi,t_P)]\sin\theta d\theta d\phi \bigg/ \int_0^{2\pi}\int_0^{\pi}N_{EX}(\theta,\phi,0)\sin\theta d\theta d\phi \tag{31}$$

$$\Delta R = \int_0^{2\pi}\int_0^{\pi}[N_{EX}(\theta,\phi,0)-N_{EX}(\theta,\phi,t_P)]\frac{1}{2}\left(3\cos^2\theta-1\right)\sin\theta d\theta d\phi \bigg/ \int_0^{2\pi}\int_0^{\pi}N_{EX}(\theta,\phi,0)\sin\theta d\theta d\phi \tag{32}$$

where

$$N_{EX}(\theta,\phi,0) = \frac{1}{\sqrt{4\pi}}\left[Y_{00}(\theta,\phi)+R_U\sqrt{5}Y_{20}(\theta,\phi)+\left\langle\alpha_{40}^U\right\rangle Y_{40}(\theta,\phi)\right] \tag{33}$$

Anisotropy and population saturation curves can be generated from (29)–(33) using a Mathematica programme, for varying S and ratios of DUMP pulse-width to ground state vibrational relaxation time (t_P/t_R) with R_U (known) and $\left\langle\alpha_{40}^U\right\rangle$ as inputs.

5. EXPERIMENTAL PROCEDURE

The experimental apparatus for STED has been described in detail elsewhere[7,8,10]. Two experimental geometries are employed; studies of Rhodamine 6G in ethylene glycol were carried out using a 90° excitation-detection geometry (figure 4A). A collinear (180°) excitation-detection geometry (figure 4B) was employed for STED measurements in 5CB which were undertaken in 75μm path length cells. Time-resolved fluorescence lifetime and anisotropy measurements at fixed PUMP-DUMP delays were performed using picosecond photon counting. Excited state population depletion measurements were obtained from dumped and undumped total fluorescence intensity decays. Fine adjustments to the PUMP and DUMP energies were made using neutral density wheels (Melles-Griot). The typical on-sample PUMP pulse energies were below 30nJ, the DUMP pulse energy was varied between 0 and 33nJ. A DUMP wavelength of 645nm was selected to minimise the effects of DUMP induced fluorescence in rhodamine 6G and 5CB.
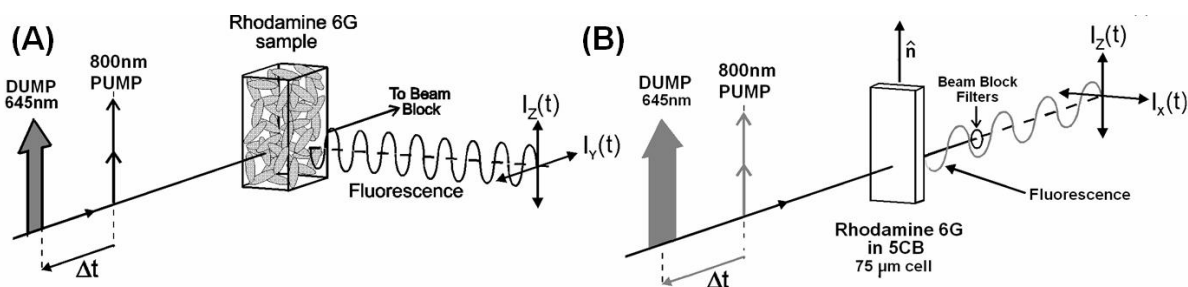

Figure 4: Excitation-detection geometries employed in the time-resolved stimulated emission depletion experiments.

6 RESULTS

Fluorescence depletion and depolarisation measurements of rhodamine 6G in ethylene glycol were undertaken using a PUMP-DUMP delay of 600ps, corresponding to an initial anisotropy R_U of 0.41. The maximum DUMP pulse energy was 33nJ; the variation in F_D and ΔR are displayed in figure 5. Fits to the data setting $\langle \alpha_{40}^U \rangle = 0$ whilst yielding an apparently reasonable agreement to the F_D data (5A1) do not reproduce the observed energy dependence of ΔR (5A2). Values of $\langle \alpha_{40}^U \rangle$ were increased with the F_D and ΔR data best fit by $\langle \alpha_{40}^U \rangle = 0.35$ and $t_P/t_R = 3$ (5B1 &5B2). For rhodamine 6G in 5CB a PUMP DUMP delay of 650ps was employed corresponding to an initial anisotropy R_U of 0.42. Measurements of F_D and ΔR up maximum DUMP energy of c.a. 19nJ were performed and the results displayed in figure 6. As with the saturation data for rhodamine 6G in ethylene glycol, setting $\langle \alpha_{40}^U \rangle = 0$ does not lead to a satisfactory fit to the ΔR data.

Values of $\langle \alpha_{40}^U \rangle$ were increased for both F_D and ΔR simulations until an optimum value was achieved. The results are shown in figure 6 where an initial hexadecapole alignment of 0.6 provides the best fit to both F_D and ΔR data, with the best value of t_P/t_R close to 1.5. In ethylene glycol and 5CB, DUMP pulsewidths of 1ps and 1.5ps were employed corresponding to ground state relaxation times of 333fs and 1ps respectively.

For rhodamine 6G in ethylene glycol the initial degree of photoselected hexadecapole alignment can be predicted from fluorescence anisotropy data via (21), these together with the predictions based on the assumption of a single element diagonal transition tensor are shown in table 1. For Rhodamine 6G predictions of the initial hexadecapole alignment based on the change in fluorescence anisotropy yield an initial value for $\langle \alpha_{40} \rangle$ of 0.77, this is considerably larger than the theoretical value of 0.38 that would be expected for a single element transition tensor. Recent circular and linearly polarised two-photon fluorescence anisotropy and absorption anisotropy measurements[23] indicate that the rhodamine 6G transition tensor has the form

$$S = \begin{bmatrix} S_{XX} & S_{XY} \\ S_{YX} & S_{YY} \end{bmatrix} \propto \begin{bmatrix} 1 & |0.1171| \\ |0.1171| & 0.1086 \end{bmatrix} \tag{34}$$

5A1

F_D

0.8
0.6
0.4
0.2
0.0

-5 0 5 10 15 20 25 30 35

E (nJ)

5A2

0.25
0.20
0.15
0.10
0.05
0.00

ΔR

t_P/t_R=1.8, 2.1, 2.3, 2.6, 3
$\langle\alpha_{40}\rangle$=0.0
S_{MAX}=7

-5 0 5 10 15 20 25 30 35

E (nJ)

5B1

t_P/t_R=3

F_D

0.8
0.6
0.4
0.2
0.0

-5 0 5 10 15 20 25 30 35

E (nJ)

5B2

t_P/t_R=3

0.25
0.20
0.15
0.10
0.05
0.00

ΔR

t_P/t_R=1.8, 2.1, 2.3, 2.6, 3
$\langle\alpha_{40}\rangle$=0.35
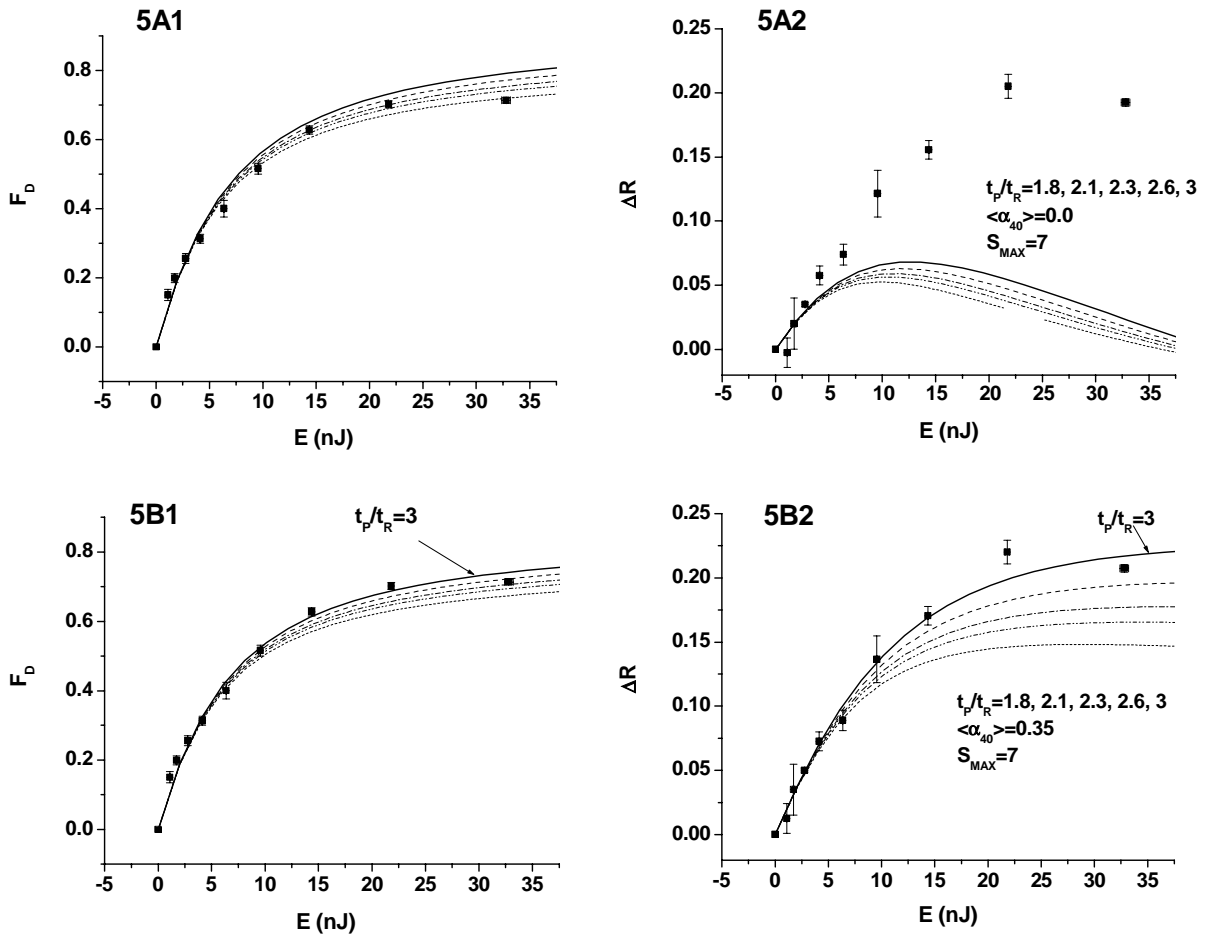S_{MAX}=7

-5 0 5 10 15 20 25 30 35

E (nJ)

Figure 5 Excited state depopulation (F_D) and depolarisation measurements for rhodamine 6G in ethylene glycol, the PUMP-DUMP separation was 600ps corresponding to an initial anisotropy R_U of 0.41. A1 and A2 show fits to the data neglecting the contribution of hexadecapole alignment, B1 and B2 show fits to the data with $\left\langle\alpha_{40}^{U}\right\rangle$=0.35, the best agreement between F_D and ΔR data is given by t_P/t_R=3.

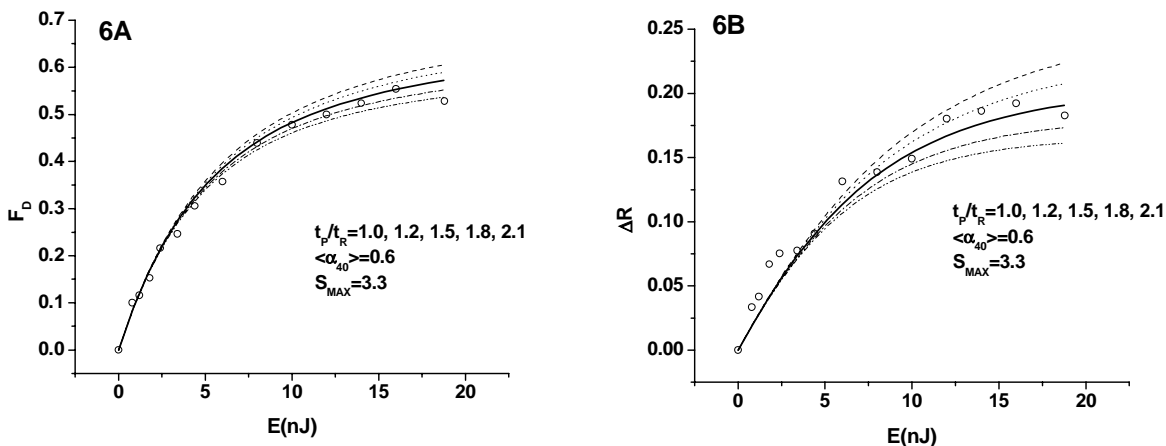*Figure 6 (A) Excited state depopulation (F_D) and (B) depolarisation measurements ΔR for rhodamine 6G in the isotropic phase of 5CB. The PUMP-DUMP separation was 600ps corresponding to an initial anisotropy R_U of 0.42. The F_D and ΔR data is best fit by simulations in which the undumped hexadecapole alignment is =0.6 and t_P/t_R=1.5.*

The divergence in the degree of photoselected hexadecapole alignment from that predicted by a single element transition tensor ($S_{ij}=\delta_{iX}\delta_{jX}$) has yet to be calculated although initial degrees of alignment greater than $(4\sqrt5)/7$ have been shown to arise from interference terms in of different sign[16,18,19]. In the case of rhodamine 6G in 5CB the value of $\left\langle\alpha_{40}^U\right\rangle$ at 650ps after excitation is 0.6. Hexadecapole alignment dynamics in a medium exhibiting bi-exponential rotational diffusion cannot be related to fluorescence anisotropy changes via simple relationships such as (21). Here predictions of $\left\langle\alpha_{40}\right\rangle$ evolution require knowledge of both the local steady-state hexadecapole alignment and the relationship between the K=2 and K=4 domain and intra-domaim relaxation times. Nonetheless without the assumption of any detailed model for the higher order diffusion dynamics it is clear that for a comparable degree of excited state alignment to that in ethylene glycol the degree of hexadecapole alignment that is present in the array 600ps after excitation is considerably larger than in ethylene glycol. If the initial value of the hexadecapole alignment is 0.77 for both molecules (i.e. solvent independent) then it is clear that hexadecapole alignment relaxation in 5CB is considerably slower than the alignment dynamics. This is somewhat surprising as the sensitivity (i.e. decay) of a higher order correlation function to angular averaging should be greater. The anisotropy of the rhodamine 6G transition tensor in 5CB is currently under investigation in our laboratory.

	Initial Anisotropy R(0)	Undumped Anisotropy R_U	$\langle\alpha_{40}^U\rangle$	$\langle\alpha_{40}(0)\rangle$	$\langle\alpha_{40}(0)\rangle$ (S_{XX} tensor)
Rhodamine 6G (ethylene glycol)	0.52	0.41	0.35	0.77	0.38
Rhodamine 6G in 5CB	0.497	0.42	0.60	(1.05)	0.38

Table 1 Initial fluorescence anisotropies (R(0)),and undumped fluorescence anisotropies (R_U) for rhodamine 6G in ethylenc glycol and 5CB, together with the calculated undumped hexadecapole alignment, the initial hexadecapole alignment is extrapolated assuming Debye diffusion dynamics; the value of 1.07 for 5CB is in brackets as Debye diffusion dynamics are not obeyed in this system.

7. CONCLUSIONS

Stimulated emission population and depolarisation measurements permit the measurement of the previously hidden degrees of excited state alignment that are created by two-photon excitation. Measurements of the degree of hexadecapole order in rhodamine 6G yield values that are substantially larger than those expected for a single element transition tensor (S_{XX}). The presence of off diagonal elements is known to yield values of the initial molecular alignment in excess of that obtained for S_{XX} alone; our results indicate that the creation of hexadecapole alignment is a highly sensitive probe of such structure. Differences between hexadecapole and alignment relaxation dynamics of rhodamine 6G in the isotropic phase of 5CB are also apparent and are the subject of ongoing study.

ACKNOWLEDGEMENTS

REFERENCES

[1] D. E. Reisner, R. W. Field, J. L. Kinsey and H-L. Dai, J. Chem. Phys. **80** 5968- 5978 1984.

[2] I. Gryczynski, J. Kusba and J. R. Lakowicz, J. Chem. Phys. **111** 89-99 1994, J. Kusba, V. Bogdanov, I. Gryczynski and J. R. Lakowicz, Biophys. J. **67** 2024-2040 1994

[3] S. A. Kovalenko, J. Ruthmann and N. P. Ernsting, J.Chem Phys. **109** 1894-1900 1998

[4] Ch. Buehler, C. Y. Dong, P. T. C. So, T. French and E. Gratton. Biophys. J **79** 536-549, 2000

[5] T. A. Klar, S. Jakobs, M. Byba, A. Egner and S. W. Hell Proc. Nat. Acad. Sci. (USA) **97** 8206 2000

[6] D. A Armoogum, A. J. Bain and R. J. Marsh, Proc. Int Soc. Opt. Eng. **4812** 45-54 2002

[7] R. J. Marsh, D. A. Armoogum and A. J. Bain, Chem. Phys. Lett. **366** 398-405 2002.

[8] D. A. Armoogum R. J. Marsh and A. J. Bain Proc. Int Soc. Opt. Eng. **5222** 34-44 (2003)

[9] A. J. Bain, R. J. Marsh and D. A. Armoogum, L. Porres O. Mongin and M. Blanchard-Desce Bio. Chem. Soc Trans **31,** 1047-1051 2003

[10] R. J. Marsh, N. D. Leonczek D. A. Armoogum L. Porres O. Mongin M. Blanchard-Desce and A. J. Bain Proc. Int Soc. Opt. Eng. **5510** 117-128 2004

[11] T. Tao Biopolymers **8** 609-632 1969

[12] C. Zannoni, A Arcioni and P Cavatorta Chem. Phys. Lipds **32**: 179-250 1983

[13] A. Szabo J. Chem. Phys. **72** 4620- 4626 1984.

[14] A. J. Bain, P. Chandna, and J. Bryant, J. Chem. Phys. **112,** 10418-10434 2000

[15] A. J. Bain, P. Chandna, and J. Bryant, J. Chem. Phys. **112** 10434-10449 2000

[16] C. Z. Wan and C. K. Johnson Chem. Phys. 179 513-531 1994

[17] P. R. Callis J. Chem .Phys. **99** 27-37 1993

[18] S. W. Pauls, J. F. Hedstrom and C. K. Johnson, Chem. Phys. **237** 205-222. 1998

[19] P. R. Callis Annu. Rev. Phys. Chem. **48** 271-297 1997

[20] B. Berne and R. Pecora *Dynamic Light Scattering* (Wiley New York 1976)

[21] E. M. Monge J. Bryant B. Obradovic A. Harsono and A. J. Bain Proc. Int Soc. Opt. Eng. **5213** 213-223 2003

[22] E. M. Monge PhD Thesis University of London 2003 (unpublished)

[23] R. J. Marsh, N. D. Leonczek D. A. Armoogum L. Porres O. Mongin M. Blanchard-Desce and A. J. Bain (to be published)